Robotic Manipulation of Thin Objects within Off-the-shelf Parallel Grippers with a Vibration Finger

Noam Nahum and Avishai Sintov[1]

School of Mechanical Engineering, Tel-Aviv University, Tel-Aviv 6997801, Israel.

Abstract

Common parallel grippers are limited to closing on an object without the ability for intrinsic in-hand manipulation. Nevertheless, parallel grippers are widely used due to their simplicity and low-cost while relying on extrinsic capabilities for manipulating the object. In this paper, a simple and low-cost mechanism is proposed for augmenting a parallel gripper with intrinsic in-hand manipulation abilities. A novel vibration-based finger was proposed where an off-the-shelf eccentric rotating mass motor along with a simple rotary actuator apply directional movement forces on a grasped thin object. The motion is based on the *stick-slip* phenomenon and exerted with no exposed moving parts. Along with the mechanism, a simple control law is proposed to manipulate the object to desired position goals and along paths. Furthermore, the ability to manipulate various objects is demonstrated. Experimental results show the ability to manipulate an object with accuracy of less than 2 mm. The experiments demonstrate the merits of the approach granting in-hand manipulation capabilities, that previously were not possible, to any parallel gripper.

Keywords: Vibration, In-hand manipulation, Parallel grippers

1. Introduction

In-hand manipulation capabilities of robotic hands are an important feature for efficient interaction with the environment. While dexterous robotic hands, such as the Shadow and the Allegro hands, are very capable, they have complex structure with many degrees-of-freedom (DOF) and, therefore, require agile sensory

[1]Corresponding author: Tel.: +972-3-6408443, e-mail: sintov1@tauex.tau.ac.il.

feedback, sophisticated control and planning to achieve robust manipulation [1]. Hence, these hands are highly expensive and not accessible for practical applications such as assembly lines or medical procedures.

Parallel jaw grippers, on the other hand, are widely used due to their simplicity, durability and low cost. They can precisely grasp almost any object of the same scale and, therefore, are ubiquitous in industrial application of material handling [2]. However, jaw grippers normally have only one DOF for opening and closing the jaws. Hence, they do not have independent in-hand manipulation capabilities. The most common manipulation approach for jaw grippers is pick-and-place where the object is placed on a surface and picked up again in a different grasp configuration [3]. However, the picking and placing can be slow and demands a large surface area around the robot.

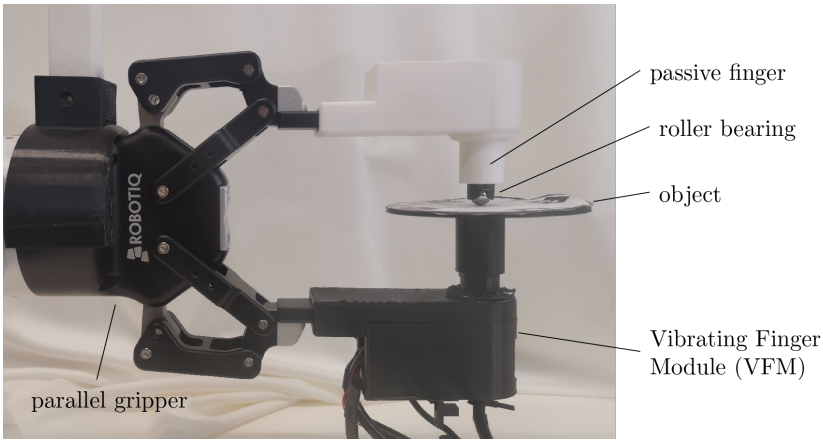

Figure 1: Prototype of the Vibratory Finger Manipulator (VFM) installed on an off-the-shelf parallel gripper.

State-of-the-art for in-hand manipulation with parallel grippers (that does not involve picking and placing) is commonly divided to extrinsic and intrinsic dexterity [4]. The former compensates for the lack of gripper DOF and involves actions of the entire robotic arm for either pushing the object against an obstacle [5, 6] or performing dynamic manipulation such as pivoting [7, 8, 9, 10, 11] or throw-and-catch [12]. A different approach leveraged gravity to control slippage between the fingers of the parallel gripper [13]. For instance, Costanzo [14] exploited a dual-arm system and tactile feedback to allow controlled slippage between the object and parallel grippers. The work of Shi et al. [15] controlled the force distribution of a pinch grasp to predict sliding directions. Similarly, Chen et al. [16]

controlled the sliding velocity of an object grasped by a parallel gripper. These methods usually require grip force control and agile sensory feedback of object pose.

In intrinsic manipulation, the available DOF of the gripper are exploited for manipulating the grasped object [17]. While jaw grippers have only one DOF, some work have been done to augment their intrinsic manipulation capabilities. Seminal work by Nagata [18] proposed six gripper mechanisms with an additional one DOF at the tip, each having an ability to either rotate or slide an object in some direction. Similarly, a passively rotating mechanism was integrated into the fingers of the gripper allowing the object to rotate between the fingers by gravity [19]. In [20], a jaw gripper tip was augmented with a two DOF transmission mechanism to re-orient and translate randomly placed screws. In [21], linear actuation was added along each of the two fingers to enable translation and twist of a grasped object. Similarly, a rolling mechanism was added to the gripper in [22] in order to manipulate a flat cable. In-hand manipulation was also enabled for a minimal underactuated gripper by employing an active conveyor surface on one finger [23]. In [24], a pneumatic braking mechanism was included to a parallel gripper in order to transition between object free-rotating and fixed phases. The above augmentation methods for parallel grippers are limited to one manipulation direction and yield bulky mechanisms that complicate the hardware.

This work explores the use of vibration for in-hand manipulation. The first known part manipulation with vibration was presented by Chladni during the 18th century using acoustic-based horizontally-vibrating plates [25]. Similarly, recent work used a single acoustic actuator to control the position of multiple objects on an horizontal plate simultaneously and independently [26]. In addition to acoustic vibrations, the use of mechanical excitation to generate vibrations and object manipulation has been widely researched [27, 28]. The work by Böhringer [29] analyzed the effect of plate oscillation frequency and the corresponding dynamic modes to the motion of an object. In [30], four linear actuators were used to generate various velocity fields across an horizontal plate. Breguet and Clavel [31] introduced the *Stick-Slip* actuators using piezo-elements to manipulate micro-components. Stick-slip is a phenomenon where contact between two surfaces is alternated between static (i.e., no relative motion) and kinetic (i.e., sliding relative each other) friction, and is caused by, for instance, applying vibrations. Baksys at el. [32] used one rotary actuator with a perpendicular axis to generate tangential forces that traverse an object across the plate. Most recently, Kopitca et al. [33] used a piezoelectric actuator to generate nonlinear vibration fields for gathering particles into a desired two-dimensional shape.

While the above works focused on manipulating arbitrary objects using vibration of an extrinsic horizontal plate, some efforts have been put to manipulate micro-robots by employing on-board vibration motors. A large effort has been put on micro-actuation techniques based on piezoelectric actuators [34, 35]. However, piezo-components are complex systems and quite expensive [36]. Hence, using the Stick-Slip principle, Vartholomeos and Papadopoulos [37] proposed to actuate a micro-robot using two simple mechanical vibration motors positioned colinearly. Such mechanism enables precise actuation with low cost hardware. The mechanism later inspired the design of the Kilobot [38] for swarming behaviour research [39].

In this paper, a novel mechanism termed *Vibratory Finger Manipulator* (VFM) is proposed. The VFM module can potentially augment the capabilities of any generic off-the-shelf parallel jaw gripper and enable it to perform in-hand manipulation of thin objects (Figure 1). The VFM is a simple and affordable vibration-based mechanism which can easily be integrated onto any parallel gripper. The motion principle is based on the *stick-slip* phenomenon where the application of vibrations enables active control of friction [31]. Such approach enables the generation of a propagation force onto an object in contact. Hence, this effect is employed using a low-cost vibration motor along with a rotary actuator to steer the force towards the required direction. Along with the mechanism, a dynamic analysis of the proposed system is provided. Furthermore, with vision-based object configuration feedback, the ability to control the motion and manipulate the object to desired goals is shown. The proposed mechanism has applications in, for example, precise manipulation of thin surgical knifes in medical procedures, robot insertion of plastic cards (e.g., credit cards) and key manipulation.

Not much work have combined mechanical grippers to the notion of vibration. However, vibration is extensively used in releasing micro- and nano-objects within a parallel gripper [40, 41, 42]. In [43], vibration was used to overcome the adhesion force of a vacuum gripper holding micro-objects. On the other hand, Honda [44] proposed a two finger gripper where each finger is comprised of an Eccentric Rotating Mass (ERM), a mass and two springs. Such gripper can hold an object of unknown weight and surface with the most suitable grasping force. Nakamura and Honda [45] proposed a multi-finger robotic hand where each finger has a vibration roller to allow uni-dimensional motion of a grasped object. Similarly, the work by Suzuki et al. [46] used vibration to control slippage of an object during gravity-based pivoting.

To summarize, the contributions of this work are as follows. First, a novel vibration-based mechanism is proposed that augments the capabilities of any stan-

Table 1: Notation and nomenclature used throughout the paper

Symbol	Meaning	Symbol	Meaning
DOF	Degrees Of Freedom	$\mathbf{g}$	Gravitation vector
VFM	Vibratory Finger Manipulator	f_ξ, f_ζ	forces on rotation axis
ERM	Eccentric Rotating Mass	$\mathbf{f}_N$	Normal force
COM	Center Of Mass	f, f_c	Forces
RMSE	Root Mean Square Error	$\mathcal{O}$	VFM coordinate frame
f_b	Initial grasp force	$\mathbf{r}$	Object COM position
$\mathcal{B}$	Manipulated object	ϕ	Object orientation
M	Mass of manipulated object	θ	Force steering angle
I	Inertia of manipulated object	τ_f	Torsional friction torque
m	ERM mass	τ_t	Net torque
l	ERM link length	γ	Static torsional friction coef.
φ	ERM rotation angle	μ	Dyn. torsional friction coef.
ω	ERM frequency	μ_s	Static friction coef.
ξ, ζ	ERM coordinate axes	μ_k	Dynamic friction coef.
$\hat{\cdot}$	Unit vector	$\mathbf{r}_g$	COM goal position
Γ	Scalar	$\mathbf{x}, \mathbf{y}, \mathbf{z}$	State vectors

dard off-the-shelf parallel gripper. The mechanism is composed of simple and low-cost hardware. Standard parallel grippers are unable to perform intrinsic in-hand manipulation. With the addition of such simple mechanism, parallel grippers are given the ability to perform in-hand manipulation of thin objects. In addition, a simple model-free controller is proposed to manipulate a grasped object to desired goal positions. The proposed system is tested and analyzed over a set of different objects. To the best of the authors' knowledge, our work is the first to combine vibration motors to in-hand manipulation for robotic hands. As a matter of convenience, Table 1 presents the nomenclature of this paper.

2. Method

2.1. Design

We leverage the ability of vibration in order to manipulate an object in contact and propose the design of the VFM module. An illustration of the VFM mechanism is seen in Figure 2. The VFM is composed of two actuators: an ERM motor and a rotary one. The ERM motor is positioned at the tip of the finger within a

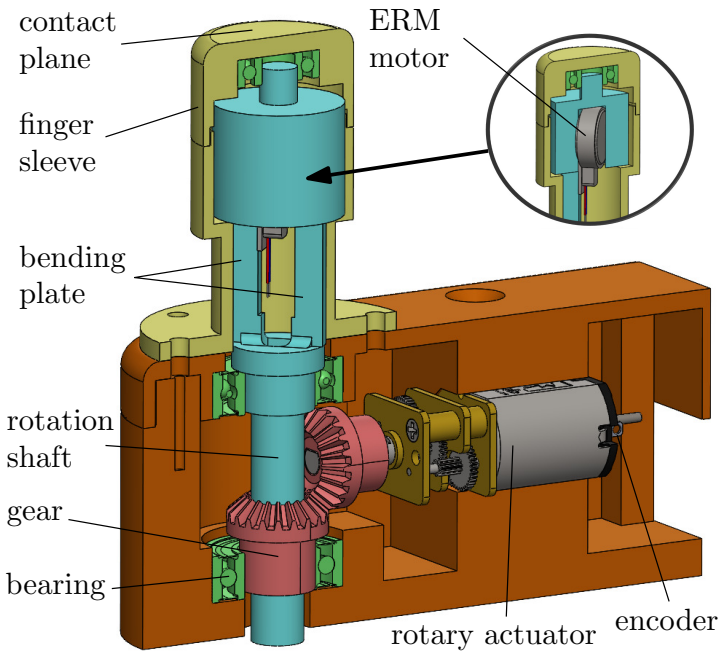

Figure 2: Section view of the Vibratory Finger Manipulator (VFM).

rotating shaft such that its axis is perpendicular to the shaft axis. The shaft is fabricated by 3D printing with a Polylactic-Acid (PLA) filament and rotates within three bearings to allow concentric motion with minimal friction. In addition, the rotating shaft includes a thin bending plate where its normal is perpendicular to the ERM axis. While a high second moment of area of the shaft (e.g., a circular profile) in the vibration direction would cause attenuation and loss of force magnitude, the bending plate with low second area moment routes the vibrational force in the direction of its normal and reduces attenuation.

The ERM motor and bending plate are covered be an elastic sleeve fabricated by 3D printing with an elastic polymer (Thermoplastic polyurethane). This configuration enables high vibrational forces at the finger pad in contact with the manipulated object while reducing attenuation. Due to this configuration, there may be some small angle deviations of the bending plate in its normal direction. Although some vibration force losses may exist, the deviations are significantly limited by the finger sleeve. Hence, the deviations are considered negligible and the motion of the plate tip is assumed to be horizontal. By rotating the ERM motor, harmonic force is generated on the plane perpendicular to the rotation axis.

The harmonic force generates the Stick-Slip effect (explained in detail below) yielding object movement. Furthermore, the sleeve is mounted to the base of the model where a rotary actuator is connected to the shaft through a bevel gear. Using an encoder, the rotary motor can rotate the shaft and control the direction of the vibrational forces.

At the opposing side of the gripper, a passive finger is fixed. A roller ball bearing is positioned at the tip of the passive finger and is in contact with the object for minimal friction. Both fingers grasp the object in some initial force f_b in direction normal to the object surface. The above mechanism provides an encapsulated vibration system to manipulate an object without exterior or exposed moving components.

2.2. Dynamic Analysis

In this Section, the motion principle of the ERM motor is analyzed, based on previous work for micro-robots [37]. Then, given object $\mathcal{B}$ with mass M and inertia moment I, the dynamic effect of the mechanism on $\mathcal{B}$ is observed.

2.2.1. Movement force

The motion mechanism of the ERM is based on a small eccentric mass m rotated by a motor through a link of length l as shown in Figure 3. The rotation is assumed to be in constant angular velocity (e.g., frequency) $\omega = \dot{\varphi}$ where φ is the angle of rotation. In such setting, forces exerted on the rotation axis in directions of the mechanisms coordinate axes ξ and ζ, while considering the orientation of the gripper, are given by

$$f_\xi = ml\omega^2 \cos\varphi + m(\hat{\xi} \cdot \mathbf{g}) \tag{1}$$

$$f_\zeta = ml\omega^2 \sin\varphi + m(\hat{\zeta} \cdot \mathbf{g}), \tag{2}$$

where $\hat{\xi}$ and $\hat{\zeta}$ are the axes vectors expressed in some global coordinates, and $\mathbf{g}$ is the gravitation vector. The dot products in (1) and (2) are the projection of the gravitational force on the $\hat{\xi}$ and $\hat{\zeta}$ axes, respectively.

The resulting vibrational forces described above are exerted on the grasped object. The normal force that is exerted on the object due to the ERM, dual-finger grip and gravitation is

$$f_N = f_\zeta + f_b + M(\hat{\zeta} \cdot \mathbf{g}). \tag{3}$$

Furthermore, force f_ξ is attenuated due to the structure of the finger, i.e., due to the elastic sleeve and bending plate. That is, the tangential force exerted on the

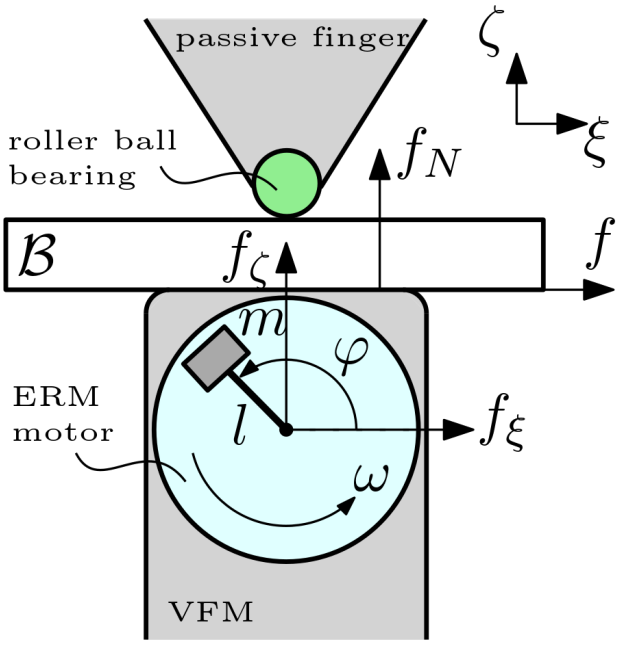

Figure 3: Illustration of the ERM rotation plane and the stick-slip effect on the object in contact.

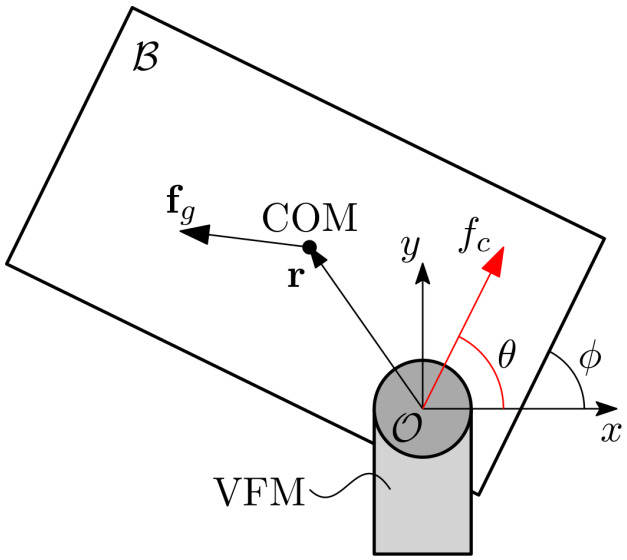

Figure 4: Illustration of vibration force f_c applied to object $\mathcal{B}$.

object is

$$f = \Gamma(f_\xi) \tag{4}$$

where $\Gamma(\cdot)$ is some unknown non-linear map [47]. The map would reduce the amplitude of the force such that $f \leq f_\xi$ while it is difficult to evaluate because of the complex structure and fabrication process.

2.2.2. Object dynamic model

Coordinate frame $\mathcal{O}$ is defined to be fixed at the center of the VFM as seen in Figure 4. Hence, the configuration of object $\mathcal{B}$ with respect to $\mathcal{O}$ is defined by the position $\mathbf{r} = (x, y, 0)^T$ of the center-of-mass (COM) and the rotation angle ϕ about the z axis, i.e., the configuration space of the $\mathcal{B}$ is $SE(2)$. The motion of $\mathcal{B}$ occurs, therefore, on plane $x - y$ of $\mathcal{O}$. Force f from (4) is exerted on the object at steering angle $\theta \in [-\pi, \pi]$ with respect to the x-axis, i.e., in direction $\hat{\mathbf{f}} = (\cos\theta, sin\theta, 0)^T$. Steering angle θ is, therefore, the action input to the system which defines the desired object direction of motion. The equations of motion that describe the sliding of the object within the gripper fingers are given by

$$M\ddot{x} = (f_c + f_g)\cos\theta \tag{5}$$

$$M\ddot{y} = (f_c + f_g)\sin\theta \tag{6}$$

$$I\ddot{\phi} = f_c\,(x\sin\theta - y\cos\theta) - (xf_{g_y} - yf_{g_x}) + \tau_f. \tag{7}$$

Vector $\mathbf{f}_g = (f_{g_x}, f_{g_y}, 0)^T$ is the projection of the gravitation force vector $M\mathbf{g}$ onto the motion plane $x - y$. That is, force $\mathbf{f}_g$ is the effect of gravitation on the planar motion and acting on the COM as seen in Figure 4. Scalar f_g is the operation of $\mathbf{f}_g$ along the direction of the vibration force and is given by the dot product $f_g = \mathbf{f_g} \cdot \hat{\mathbf{f}}$. Equation (7) is acquired from the conservation of momentum where the first term at the right hand side is the z component of the cross product $\mathbf{r} \times \hat{\mathbf{f}}$. Similarly, the second term is the z component of the cross product $\mathbf{r} \times \mathbf{f}_g$ and is the torque generated by the gravitational force. Scalar τ_f is the torsional friction at the contact point and is given by

$$\tau_f = \begin{cases} -\gamma f_N sgn(\tau_t), & |\dot{\phi}| = 0 \\ -\mu f_N sgn(\dot{\phi}), & |\dot{\phi}| > 0, \end{cases} \tag{8}$$

where τ_t is the net torque acting on the contact point in order to maintain static equilibrium, and $\gamma, \mu > 0$ are the static and dynamic coefficient of torsional friction [48, 49].

Force f_c is dependent of whether the object and finger are in *stick* mode (i.e., static friction) or in *slip* mode (i.e., relative motion with kinetic friction), and is given by

$$f_c = \begin{cases} f, & |f + f_g| \leq \mu_s |f_N| \\ f - \mu_k f_N, & |f + f_g| > \mu_s |f_N|, \end{cases} \tag{9}$$

where μ_s and μ_k are the static and kinetic coefficients of friction, respectively, between the finger and object. In the slip mode, the object will move in direction $\hat{\mathbf{f}}$, when $f_g > 0$ and f_g is assisting f_c; or when $f_g < 0$ and $|f_c| > |f_g|$. The latter case depends on the friction coefficient and grip force. Hence, inclined manipulation under the effect of gravity will be demonstrated in the experimental section.

Figure 5 presents a one-dimensional simulated example (i.e., solely along the x-axis) of the motion. In this example, the angular velocity ω is in the positive direction. While $f_N > f_b$, the eccentric mass is at the highest point ($\varphi = 90°$) of the cycle leading to high frictional force. This is the stick phase in which the f force is applied to the object in the positive direction and, thus, generating displacement of both finger and object in the positive x direction. Similarly, when the mass is at its lowest point ($\varphi = -90°$), the normal force is the lowest. When the magnitude of the normal force declines, the f force switches direction yielding relative slip between the finger and object (while the finger experiences negative displacement). Consequently, the displacement in the positive direction is larger

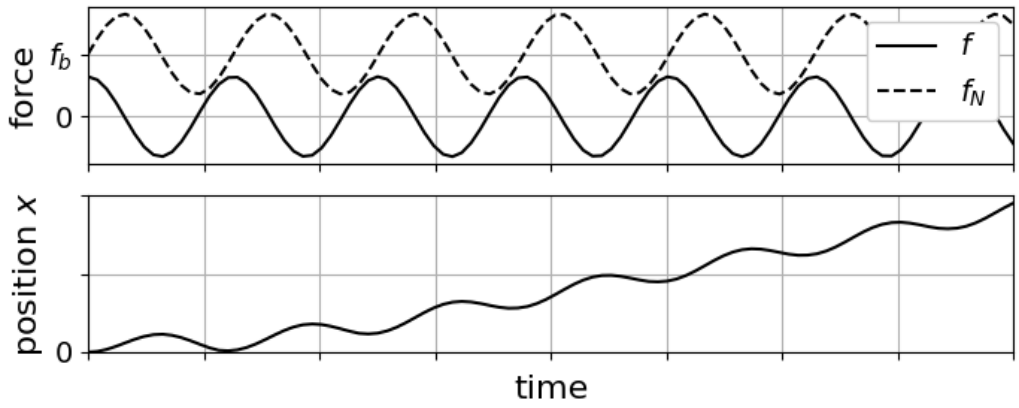

Figure 5: A one-dimensional example of motion: (top) Tangential and normal forces, f and f_N, applied to the object and (bottom) displacement of object along the x direction.

than the negative one, leading to cumulative net displacement in the positive direction. Excitation of negative ω would force negative displacement in the same manner.

A gripper with a VFM finger has a one-DOF actuation space (i.e., steering angle θ) while the object configuration is of three-DOF (i.e., x, y and ϕ). Hence, the system is considered underactuated where the entire configuration of the arm cannot be fully controlled. The next section discusses position control of the object while maintaining constant orientation. Controlling object position along with its orientation requires manipulation planning which we leave out of the scope of this paper.

2.3. Control

Consider the problem of manipulating the COM of the object to a goal position $\mathbf{r}_g = (x_g, y_g, 0)^T$ relative to $\mathcal{O}$. While the control of the COM position is formulated, the position of any other point on the object can be controlled instead as will be shown in the experiments. System (5)-(7) can be formulated in the state space as

$$\dot{\mathbf{x}} = F(\mathbf{x}, \theta) \tag{10}$$

where $\mathbf{x} = (x_1, \ldots, x_6)^T \in \mathbb{R}^6$, $x_1 = x$, $x_2 = \dot{x}$, $x_3 = y$, $x_4 = \dot{y}$, $x_5 = \phi$, $x_6 = \dot{\phi}$,

$$F(\mathbf{x}, \theta) = \begin{pmatrix} x_2 \\ \frac{f_a}{M} \cos\theta \\ x_4 \\ \frac{f_a}{M} \sin\theta \\ x_6 \\ \frac{f_c}{I}(x_1 \sin\theta - x_3 \cos\theta) - (x_1 f_{g_x} - x_3 f_{g_y}) + \tau_f \end{pmatrix}, \tag{11}$$

and $f_a = f_c + f_g$. While having a sinusoidal behaviour, force f_c is assumed to be constant and positive for control purpose. Hence, force f_c pushes the object in direction defined by control input angle θ. Further, the state vector can be decomposed as $\mathbf{x} = (\mathbf{y}, \mathbf{z})^T$ where $\mathbf{y} = (x_1, x_2, x_3, x_4)^T \in \mathbb{R}^4$ and $\mathbf{z} = (x_5, x_6)^T \in \mathbb{R}^2$ correspond to linear and angular motion of the object, respectively. Therefore, system (10) can now be represented as

$$\dot{\mathbf{y}} = Y(\mathbf{y}, \theta) \tag{12}$$

$$\dot{\mathbf{z}} = Z(\mathbf{z}, \theta) \tag{13}$$

where $Y : \mathbb{R}^4 \times \mathbb{R} \to \mathbb{R}^4$ and $Z : \mathbb{R}^2 \times \mathbb{R} \to \mathbb{R}^2$.

Consider the following Lyapunov candidate function [50]

$$V(\mathbf{y}) = \frac{1}{2}(x_1 - x_g)^2 + \frac{1}{2}(x_3 - y_g)^2 + \frac{1}{2}x_2^2 + \frac{1}{2}x_4^2 \tag{14}$$

where $V(\mathbf{y}) > 0$ for $\mathbf{y} \neq \mathbf{y}_g$ with $\mathbf{y}_g = (x_g, 0, y_g, 0)^T$ as the goal $\mathbf{y}$-state. Substituting (12) to the time derivative of V gives

$$\dot{V}(\mathbf{y}) = (x_1 - x_g)x_2 + (x_3 - y_g)x_4 + x_2 \frac{f_a}{M} \cos\theta + x_4 \frac{f_a}{M} \sin\theta. \tag{15}$$

Having $\lambda > \frac{f_a}{M}$ for some $\lambda > 0$ and choosing

$$\cos\theta = -\lambda(x_1 - x_g), \quad \sin\theta = -\lambda(x_3 - y_g) \tag{16}$$

or

$$\tan\theta = \frac{y_g - x_3}{x_g - x_1}, \tag{17}$$

we get that

$$\dot{V}(\mathbf{y}) = \left(\frac{f_a}{M} - \lambda\right)(x_2 \cos\theta + x_4 \sin\theta). \tag{18}$$

Since $\dot{x}\cos\theta > 0$ and $\dot{y}\sin\theta > 0$ (or $sgn(\dot{x}) = sgn(\cos\theta)$ and $sgn(\dot{y}) = sgn(\sin\theta)$), it must be that

$$\dot{V}(\mathbf{y}) \leq 0. \tag{19}$$

According to partial stability theorem [51], system (10) is $\mathbf{y}$-stable. Therefore, by applying controller

$$\theta = \arctan\left(\frac{y_g - x_3}{x_g - x_1}\right), \tag{20}$$

with $\lambda > \frac{f_a}{M}$, and as long as $x_2, x_4 \neq 0$, the Lyapunov function decreases and the system is driven to $\mathbf{y}_g$.

The $\mathbf{y}$-stability of the system means that control law (20) will take sub-system $Y(\mathbf{y}, \theta)$ to position $(x_g, y_g, 0)^T$. However, applying the control to (7) yields

$$\ddot{\phi} = \frac{1}{M}\left[f_c(x_1 y_g - x_3 x_g) - (x_1 f_{g_x} - x_3 f_{g_y}) + \tau_f\right]. \tag{21}$$

Hence, the object would rotate by the effect of the controller and sub-system $Z(\mathbf{z}, \theta)$ cannot be controlled. Nevertheless, rotation would not occur if the object is at a position satisfying $xy_g - yx_g = 0$ and $\tau_f = x_1 f_{g_x} - x_3 f_{g_y}$. That is, rotation will not occur if the object moves on a line connecting the COM and the goal, and when the object is grasped tight enough by the normal force f_N to resist gravitational torque (this is easily done by applying sufficient grip force f_b and demonstrated in the experiments). In such case, motion is exerted towards or away from the COM, no torque is applied on the object and, therefore, the object will not rotate. If no rotation is desired when moving to some goal $(x_g, y_g, 0)^T \neq (0, 0)$, controlling the motion through the COM is proposed. That is, an intermediate goal $(0, 0)$ is added prior to moving to $(x_g, y_g, 0)^T$ and, thus, moving only on rotation-free lines.

3. Experiments

A prototype of the VFM was built as described in Section 2.1. The VFM includes an ERM vibration motor $10 \times 3.4\ mm$ by Pololu. We note that physical parameters of the ERM such as m and l are not specified by the manufacturer. The VFM was further installed on a Robotiq 2F-85 parallel gripper while the gripper is mounted on a Kinova Gen3 arm as seen in Figure 6. It is noted that the VFM can be installed on any parallel gripper with no regards to its closing mechanism. Also, the Robotiq 2F-85 gripper cannot provide feedback about the closing force f_b and, therefore, the gripper was closed manually on the object to some arbitrary force.

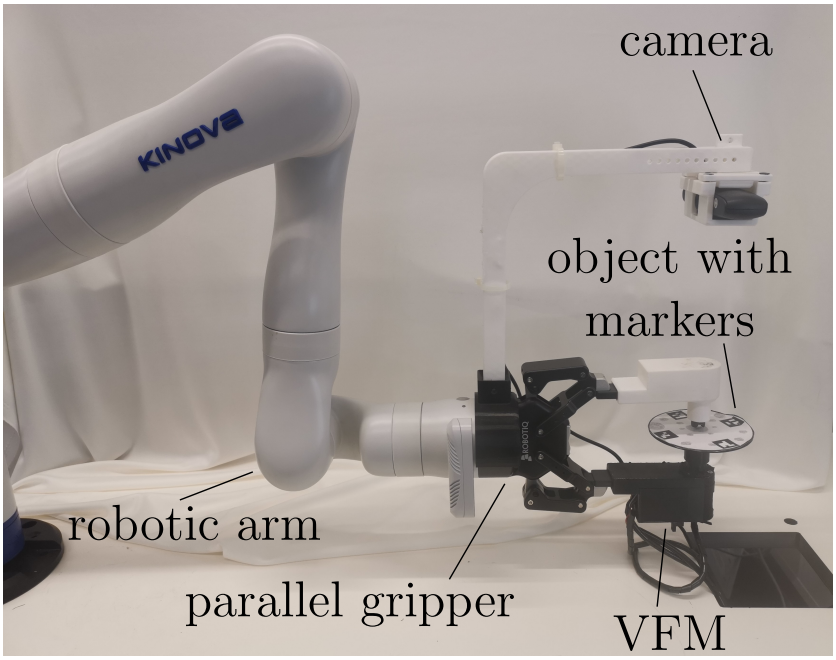

Figure 6: Experimental setup where the VFM is mounted on a Robotiq parallel gripper.

Furthermore, a camera was positioned on top of the system to track the ArUco [52] markers on the moving object. The camera provides feedback stream of object position and orientation in real-time and in frequency of 60 Hz. Aruco markers provide, within the working distance of the experiment, position and orientation errors of approximately $1.5\ mm$ and 1°, respectively [53, 54]. We first analyze the manipulation of a circular thin object printed with PLA of weight 14.84 grams and thickness 2 mm. The manipulation of other objects is later observed. All experiment videos can be seen in the supplementary material.

3.1. Mechanism Analysis

The behaviour of the mechanism with regards to certain parameters is initially observed including vibration frequency, gripper inclination and various manipulated objects. For each of the tests, object mean velocity over a sequence of 200 random steps exerted by the VFM is reported. A sequence of positions was recorded and the velocity was computed by second order backward differentiation. First, velocity of the object is observed with regards to the frequency of the ERM. Figure 7 shows results in which object velocity clearly increases with higher frequency. Hence, one can also tune the frequency in order to control mov-

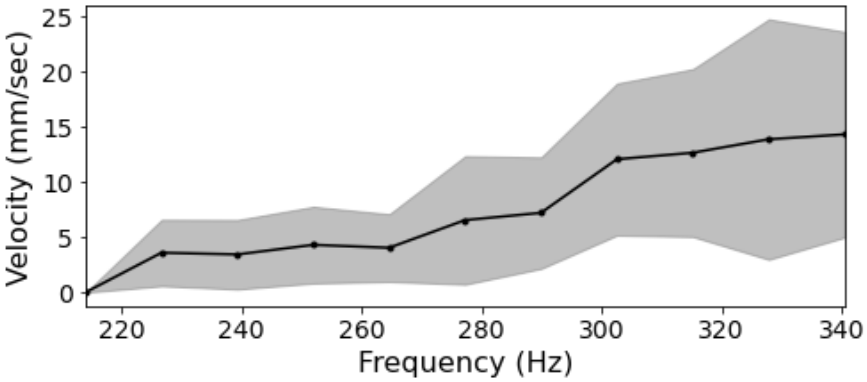

Figure 7: Mean object velocity with regards to the frequency of the vibration motor.

ing velocity. Note that the velocities also depend on the attenuation of the gripper structure derived from fabrication, material and geometry.

Next, the mean velocity of the object with regards to gripper inclination is analyzed. For such, random paths were recorded while changing the gripper angle using the robotic arm. Figure 8 shows results for mean and standard deviation object velocities with regards to the inclination angle. A rather low grip force f_b was applied on the object by the gripper between angles 0° to 25°. Above 25° inclination, the object began to slide due to gravitation. Hence, an higher gripping force was applied to increase friction. For inclination angles larger than 60°, the gripper failed to generate continuous motion of the object as the vibration force was not strong enough. Having a stronger ERM should allow working in steeper angles. It is noted that rotation due to gravitation when not applying vibration was not observed and static equilibrium was maintained by τ_f (as discussed in Section 2.3). Hence, grip force f_b was sufficient while not interfering with vibration control.

3.2. Control Evaluation

In this section, the use of control law (20) is experimented to manipulate the object to desired goal positions. The control of the COM motion directly to desired goals and through the origin are tested. Table 2 shows performance parameters for the two control strategies over 100 trials. For each trial, a desired goal was randomly chosen and motion was initiated from the reached point of the previous trial. The COM is declared to reach the target if it is within 2 mm of the goal position. This distance tolerance is defined based on the position measurement error

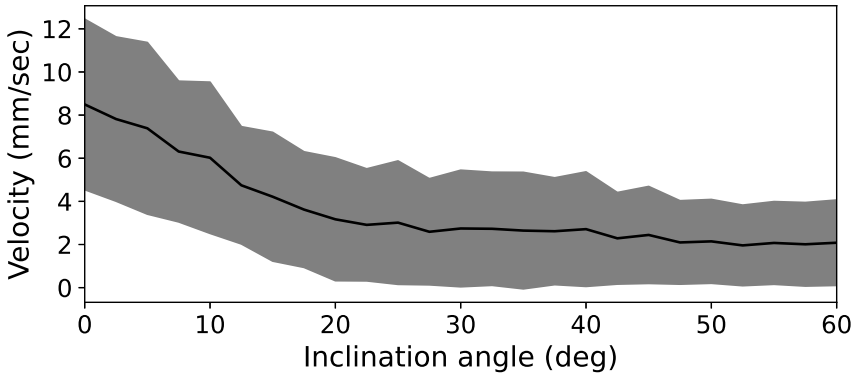

Figure 8: Mean object velocity with regards to the inclination angle of the gripper.

Table 2: Performance parameters of controller (20) directly to the goal or through the origin

		Direct	via origin
Mean error	(mm)	1.58±0.49	1.47±0.54
Mean angle change	(deg)	11.40±15.62	4.27±4.34
Mean path length	(mm)	63.75±42.86	66.55±36.48

of the system described above. When the COM reaches the current goal, vibration is terminated and motion stops instantly due to stick attenuation. Controlled motion is then applied to the next random goal. Results show that the mean final error is low and less than 2 mm for both methods. While relatively low, the error is significantly affected by the resolution of the ArUco marker tracking as discussed above, and can be reduced in future work with a designated sensing alternative. Note also that explicit knowledge of friction parameters between the gripper and objects are not required for the controller to reach desired targets.

Moving through the origin is shown to reduce the mean angle change by approximately 62%. When moving directly to the goal, torques are exerted on the object yielding a curved path as seen in Figure 9. On the other hand, control through the origin constrains forces to be nearly along a line passing through the origin leading to lower torques on the object. Hence, the paths are less curved as seen in Figure 10. Evidently, Table 2 shows that the mean lengths of paths passing and not passing through the origin are approximately similar. Position responses corresponding to manipulations in Figures 9 and 10 are seen in Figures 11 and 12, respectively.

Using the control law, path tracking was also implemented along small-sized

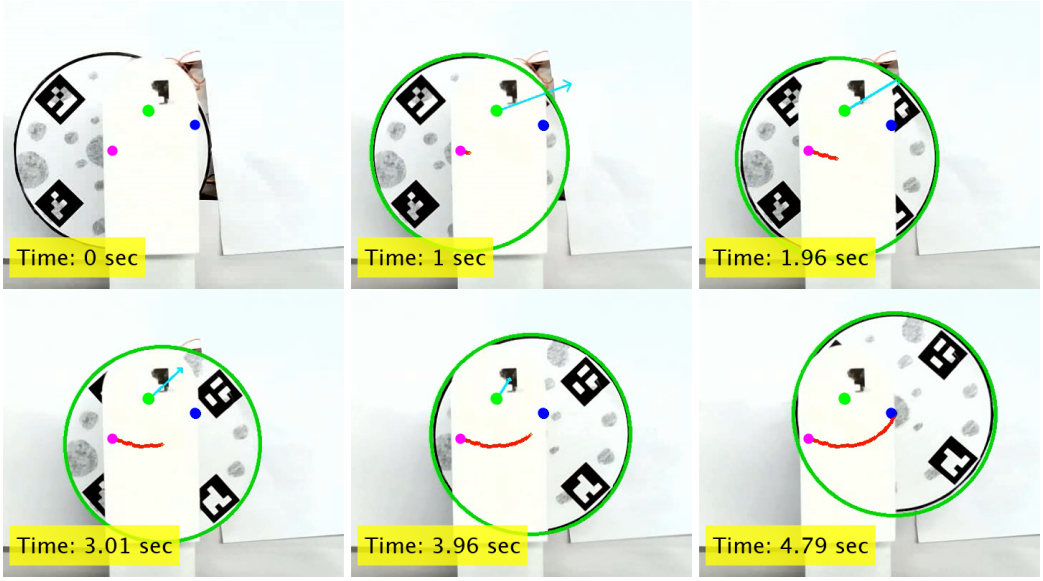

Figure 9: Manipulating the COM of a disk from an initial position (magenta marker) to a goal position (blue marker). The disk reached the goal with an accuracy of 1.93 mm error and 9.94^o orientation change.

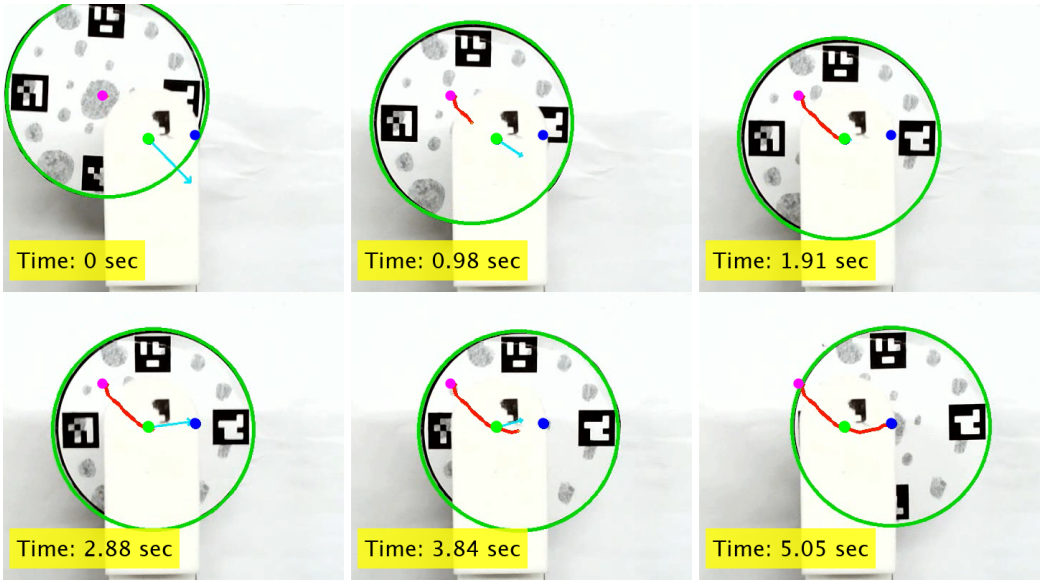

Figure 10: Manipulating the COM of a disk from an initial position (magenta marker) to a goal position (blue marker) through the origin (green marker). The disk reached the goal with an accuracy of 2 mm error and 4.39^o orientation change.

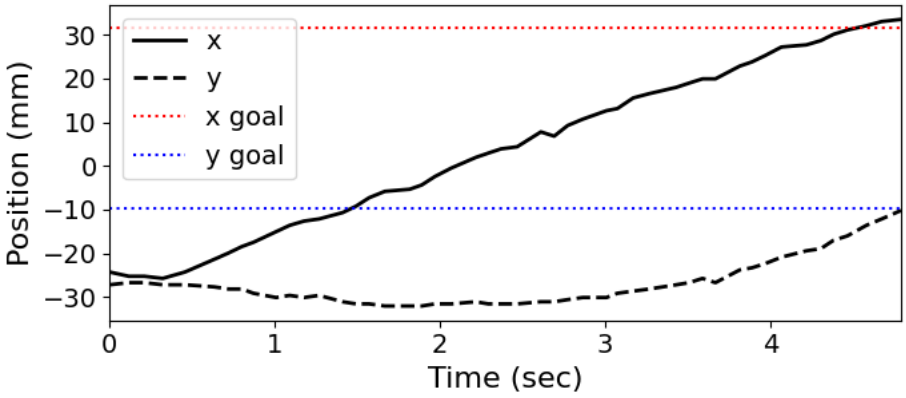

Figure 11: Position path of the disk seen in Figure 9 with respect to time.

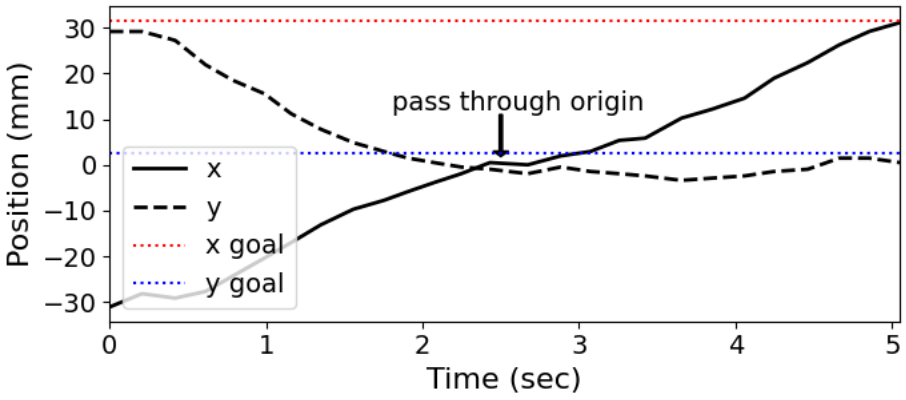

Figure 12: Position path of the disk seen in Figure 10 with respect to time.

Table 3: Tracking accuracy along a path

	Size (mm)	Tracking error (mm)
Rectangular	15×15	1.73±0.50
Circular	9 (radius)	1.99±0.31

Table 4: Performance parameters for various manipulated objects

Object	Thickness (mm)	Weight (g)	Velocity (mm/sec)	Accuracy (mm)
Utility Knife	0.2	4.68	9.7±1.22	2.01±0.38
Ruler	0.2	10.43	1.95±0.1	2.56±0.21
ID card	0.6	3.77	12.95±20.35	1.82±1.17
Paper sheet	0.05	0.71	1.41±1.55	2.5±0.2
Paperboard	0.1	1.00	1.84±1.39	2.15±0.59
Single wall cardboard	3.8	3.1	0	-

paths. Each path was discretized to 60 points. Tracking was performed with a moving intermediate goal point, i.e., a simple "follow-the-carrot" scheme, where the next intermediate point is set to be the goal once the object reaches the current one. Table 3 presents path sizes and average Root Mean Square Error (RMSE) for tracking rectangular and circular paths. Figures 13 and 14 show snapshots of tracking both paths. Results demonstrate the ability to track paths with high accuracy.

3.3. Other objects

To demonstrate the manipulation of various objects, six everyday objects were tested. The set of objects, seen in Figure 15, includes a stainless steel utility knife, a stainless Steel ruler, a plastic ID card, a paper sheet, a paperboard and a single wall cardboard. Weight and thickness of the objects along with experimental results are seen in Table 4. The results include mean and standard deviation for motion velocity and control error. The results show that smooth objects (i.e., utility knife and ID card) move faster than objects with rougher surface texture. Due to low kinetic friction, force f_c is stronger as seen in (9) yielding higher velocity. However, local deformation on the cardboard caused by gripper clamping prevented it from moving while only rotating about the contact point. In the control experiment, the attached marker on the object (not on the COM) was driven to ten desired goals showing good accuracy for all objects.

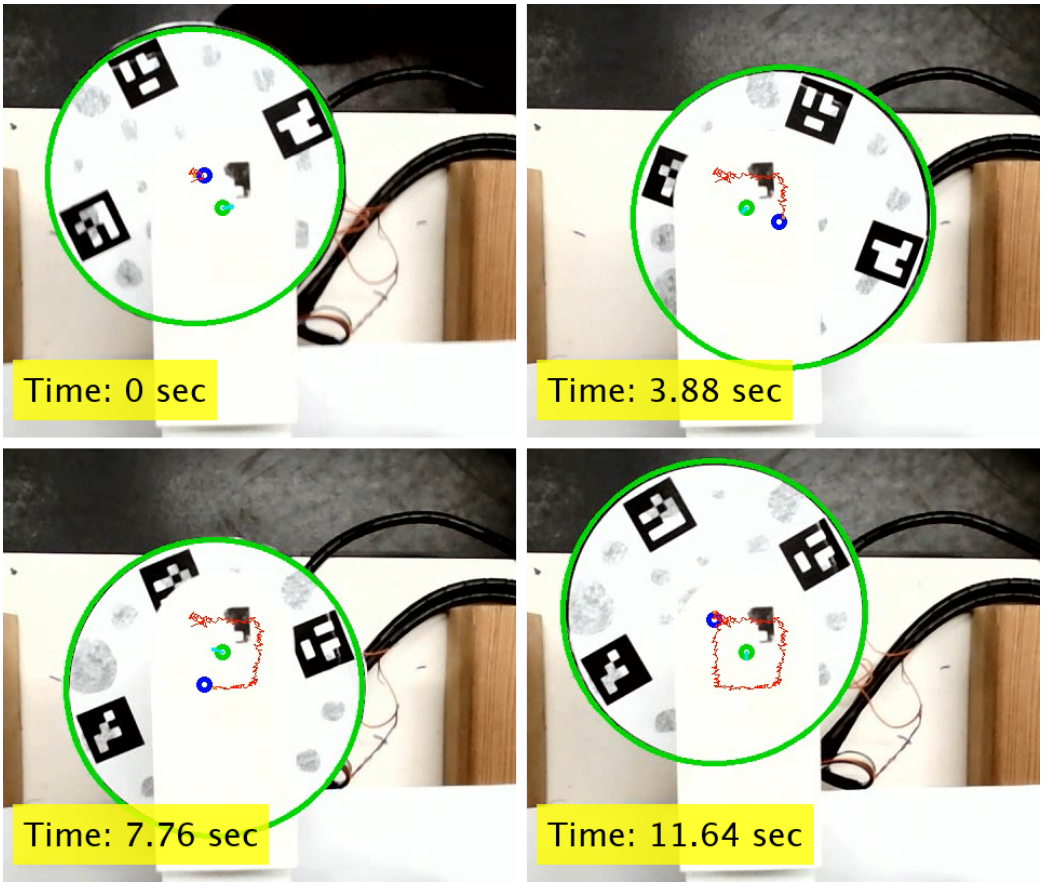

Figure 13: Manipulating the COM of a disk along a rectangular path (red path).

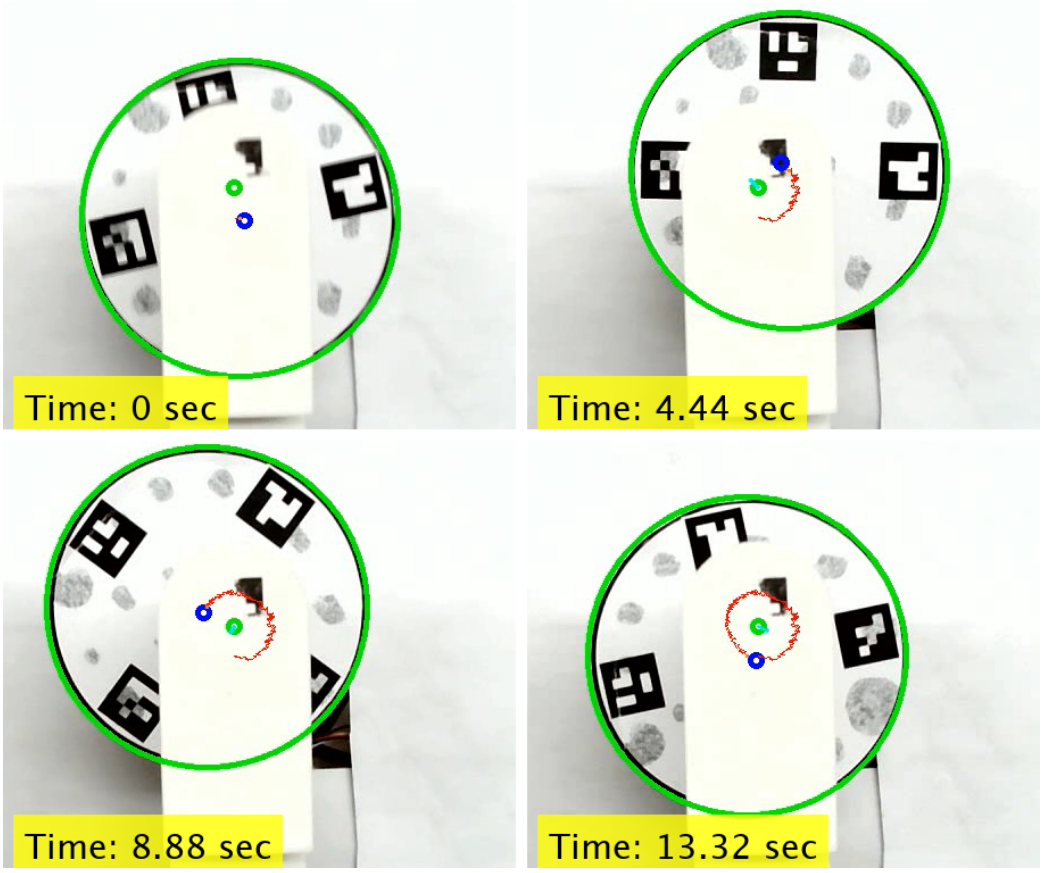

Figure 14: Manipulating the COM of a disk along a circular path (red path).

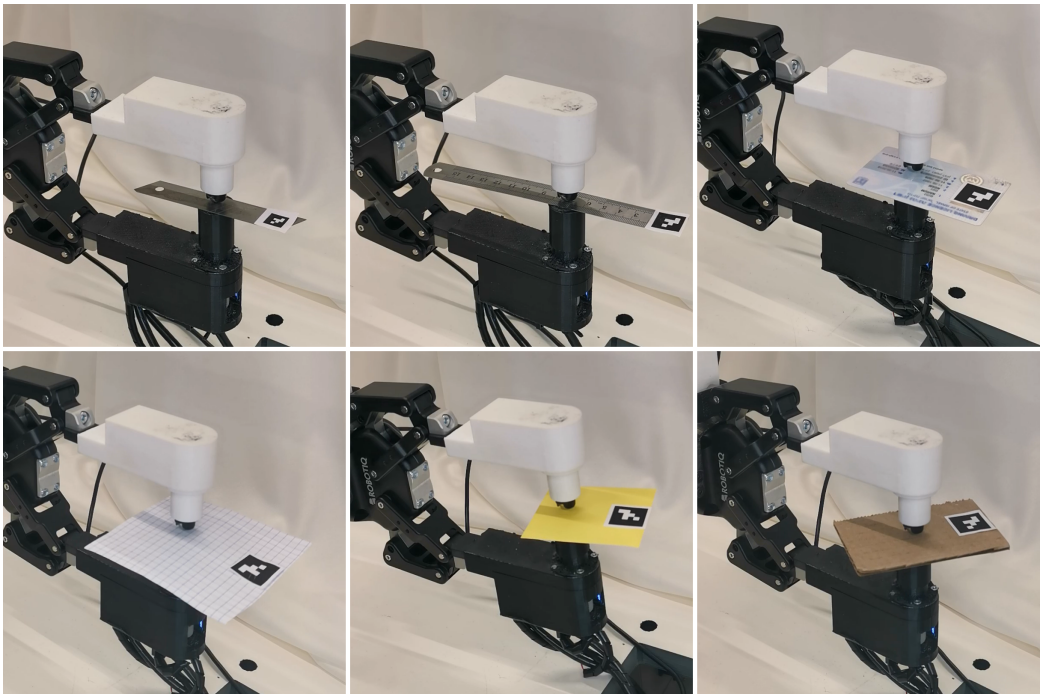

Figure 15: Manipulating various objects including (from top left): utility knife, ruler, ID card, paper sheet, paperboard and single wall cardboard.

4. Conclusions

In this paper, a novel vibration-based mechanism was presented for in-hand manipulation of thin objects. The mechanism can augment parallel grippers which alone do not have intrinsic in-hand manipulation capabilities. The proposed mechanism is based on the stick-slip phenomenon yielding a simple and low-cost solution. By having a finger comprised of an off-the-shelf vibration motor and a rotary actuator, a force can be exerted on a grasped object in a desired direction. Then, by applying a simple control law, the object can be manipulated to a desired position goal or track a path with high accuracy. A set of experiments was presented including accuracy with regards to frequency and gripper inclination angle, control behaviour and manipulation of various objects. The results show high accuracy and feasibility to objects of different material and texture.

As discussed on Section 2.2.2, the proposed mechanism is underactuated and demonstrated the ability to control the position of the object. However, controlling the orientation of the object would require planned maneuvers while considering the applied torques. For instance, future work can apply a Model Predictive Control where a motion planner constantly plans paths to a goal in $SE(2)$ based on the dynamic model. Another alternative is a gravity-assisted approach where the object is pivoted with controlled inclination of the gripper. Future work may also consider identifying the multiple vibration modes of the system to better control the motion of various objects. Furthermore, the current sensing is limited by the accuracy of the ArUco markers while also dependent on camera line-of-sight. Hence, future work could consider an on-board sensing module that can combine visual perception and odometry. Adaptive velocity control may also be implemented to reduce the velocity when approaching the vicinity of the goal for finer position tuning.

Funding

This research did not receive any specific grant from funding agencies in the public, commercial, or not-for-profit sectors.

References

[1] K. Hertkorn, M. A. Roa, C. Borst, Planning in-hand object manipulation with multifingered hands considering task constraints, in: IEEE International Conference on Robotics and Automation, 2013, pp. 617–624.

[2] M. Guo, D. V. Gealy, J. Liang, J. Mahler, A. Goncalves, S. McKinley, J. A. Ojea, K. Goldberg, Design of parallel-jaw gripper tip surfaces for robust grasping, in: 2017 IEEE International Conference on Robotics and Automation (ICRA), 2017, pp. 2831–2838.

[3] A. Zeng, S. Song, K.-T. Yu, E. Donlon, F. R. Hogan, M. Bauza, D. Ma, O. Taylor, M. Liu, E. Romo, N. Fazeli, F. Alet, N. C. Dafle, R. Holladay, I. Morena, P. Qu Nair, D. Green, I. Taylor, W. Liu, T. Funkhouser, A. Rodriguez, Robotic pick-and-place of novel objects in clutter with multi-affordance grasping and cross-domain image matching, in: IEEE International Conference on Robotics and Automation (ICRA), 2018, pp. 3750–3757.

[4] A. Billard, D. Kragic, Trends and challenges in robot manipulation, Science 364 (6446) (2019).

[5] N. C. Dafle, A. Rodriguez, R. Paolini, B. Tang, S. S. Srinivasa, M. Erdmann, M. T. Mason, I. Lundberg, H. Staab, T. Fuhlbrigge, Extrinsic dexterity: In-hand manipulation with external forces, in: 2014 IEEE International Conference on Robotics and Automation (ICRA), 2014, pp. 1578–1585.

[6] N. Chavan-Dafle, R. Holladay, A. Rodriguez, Planar in-hand manipulation via motion cones, The International Journal of Robotics Research 39 (2-3) (2020) 163–182.

[7] F. E. Viña B., Y. Karayiannidis, K. Pauwels, C. Smith, D. Kragic, In-hand manipulation using gravity and controlled slip, in: IEEE/RSJ International Conference on Intelligent Robots and Systems (IROS), 2015, pp. 5636–5641.

[8] F. E. Viña B., Y. Karayiannidis, C. Smith, D. Kragic, Adaptive control for pivoting with visual and tactile feedback, in: IEEE International Conference on Robotics and Automation (ICRA), 2016, pp. 399–406.

[9] A. Sintov, A. Shapiro, Swing-up regrasping algorithm using energy control, in: IEEE International Conference on Robotics and Automation (ICRA), 2016, pp. 4888–4893.

[10] A. Sintov, O. Tslil, A. Shapiro, Robotic swing-up regrasping manipulation based on impulse-momentum approach and cLQR control, IEEE Transactions on Robotics 32 (5) (2016) 1079–1090.

[11] S. Cruciani, C. Smith, Integrating path planning and pivoting, in: IEEE/RSJ International Conference on Intelligent Robots and Systems (IROS), 2018, pp. 6601–6608.

[12] A. Sintov, A. Shapiro, Dynamic regrasping by in-hand orienting of grasped objects using non-dexterous robotic grippers, Robotics and Computer-Integrated Manufacturing 50 (2017) 114 – 131.

[13] M. Costanzo, G. De Maria, C. Natale, Dual-arm in-hand manipulation with parallel grippers using tactile feedback, in: International Conference on Advanced Robotics (ICAR), 2021, pp. 942–947.

[14] M. Costanzo, Control of robotic object pivoting based on tactile sensing, Mechatronics 76 (2021) 102545.

[15] J. Shi, J. Z. Woodruff, P. B. Umbanhowar, K. M. Lynch, Dynamic in-hand sliding manipulation, IEEE Transactions on Robotics 33 (4) (2017) 778–795.

[16] Y. Chen, C. Prepscius, D. Lee, D. D. Lee, Tactile velocity estimation for controlled in-grasp sliding, IEEE Robotics and Automation Letters 6 (2) (2021) 1614–1621.

[17] S. Cruciani, C. Smith, D. Kragic, K. Hang, Dexterous manipulation graphs, in: IEEE/RSJ International Conference on Intelligent Robots and Systems (IROS), 2018, pp. 2040–2047.

[18] K. Nagata, Manipulation by a parallel-jaw gripper having a turntable at each fingertip, in: IEEE International Conference on Robotics and Automation, 1994, pp. 1663–1670 vol.2.

[19] H. Terasaki, T. Hasegawa, Motion planning of intelligent manipulation by a parallel two-fingered gripper equipped with a simple rotating mechanism, IEEE Transactions on Robotics and Automation 14 (2) (1998) 207–219.

[20] J. Zhao, X. Jiang, X. Wang, S. Wang, Y. Liu, Assembly of randomly placed parts realized by using only one robot arm with a general parallel-jaw gripper, 2020, pp. 5024–5030.

[21] S. Zuo, J. Li, M. Dong, Design, modeling, and manipulability evaluation of a novel four-dof parallel gripper for dexterous in-hand manipulation, Journal of Mechanical Science and Technology 35 (2021) 1–16.

[22] J. Chapman, G. Gorjup, A. Dwivedi, S. Matsunaga, T. Mariyama, B. MacDonald, M. Liarokapis, A locally-adaptive, parallel-jaw gripper with clamping and rolling capable, soft fingertips for fine manipulation of flexible flat cables, in: IEEE International Conference on Robotics and Automation (ICRA), 2021, pp. 6941–6947.

[23] In-Hand Manipulation Primitives for a Minimal, Underactuated Gripper With Active Surfaces, Vol. Volume 5A: 40th Mechanisms and Robotics Conference of International Design Engineering Technical Conferences and Computers and Information in Engineering Conference.

[24] I. H. Taylor, N. Chavan-Dafle, G. Li, N. Doshi, A. Rodriguez, Pnugrip: An active two-phase gripper for dexterous manipulation, in: IEEE/RSJ International Conference on Intelligent Robots and Systems (IROS), 2020, pp. 9144–9150.

[25] E. Chladni, Entdeckungen über die Theorie des Klanges, no. 1, Bey Weidmanns erben und Reich, 1787.

[26] Q. Zhou, V. Sariola, K. Latifi, V. Liimatainen, Controlling the motion of multiple objects on a chladni plate, Nature Communication 7 (12764) (2016).

[27] W. Y. Du, S. L. Dickerson, Modelling and control of a novel vibratory feeder, in: IEEE/ASME International Conference on Advanced Intelligent Mechatronics, 1999, pp. 496–501.

[28] M. Mayyas, Parallel manipulation based on stick-slip motion of vibrating platform, Robotics 9 (4) (2020).

[29] K. Böhringer, V. Bhatt, K. Goldberg, Sensorless manipulation using transverse vibrations of a plate, Vol. 2, 1995, pp. 1989 – 1996.

[30] D. Reznik, J. Canny, A flat rigid plate is a universal planar manipulator, in: Proceedings IEEE International Conference on Robotics and Automation, Vol. 2, 1998, pp. 1471–1477 vol.2.

[31] J. Breguet, R. Clavel, Stick and slip actuators: design, control, performances and applications, in: Proceedings of the International Symposium on Micromechatronics and Human Science, 1998, pp. 89–95.

[32] B. Baksys, K. Ramanauskytė, A. Povilionis, Vibratory manipulation of elastically unconstrained part on a horizontal plane, Mechanika 75 (1) (2009).

[33] A. Kopitca, K. Latifi, Q. Zhou, Programmable assembly of particles on a chladni plate, Science Advances 7 (39) (2021) eabi7716.

[34] F. Schmoeckel, S. Fatikow, Smart flexible microrobots for scanning electron microscope (sem) applications, Journal of Intelligent Material Systems and Structures 11 (3) (2000) 191–198.

[35] V. Shrikanth, K. R. Y. Simha, M. S. Bobji, Frictional force measurement during stick-slip motion of a piezoelectric walker, in: IEEE International Conference on Industrial Technology, 2015, pp. 1463–1468.

[36] P. Vartholomeos, K. Mougiakos, E. Papadopoulos, Driving principles and hardware integration of microrobots employing vibration micromotors, in: IEEE/ASME international conference on advanced intelligent mechatronics, 2007, pp. 1–6.

[37] P. Vartholomeos, E. Papadopoulos, Analysis, design and control of a planar micro-robot driven by two centripetal-force actuators, in: Proceedings IEEE International Conference on Robotics and Automation, 2006, pp. 649–654.

[38] M. Rubenstein, C. Ahler, N. Hoff, A. Cabrera, R. Nagpal, Kilobot: A low cost robot with scalable operations designed for collective behaviors, Robotics and Autonomous Systems 62 (7) (2014) 966 – 975.

[39] M. Rubenstein, A. Cornejo, R. Nagpal, Programmable self-assembly in a thousand-robot swarm, Science 345 (6198) (2014).

[40] H. Demaghsi, H. Mirzajani, H. B. Ghavifekr, Design and simulation of a novel metallic microgripper using vibration to release nano objects actively, Microsystem technologies 20 (1) (2014) 65–72.

[41] Z. Long, J. Zhang, Y. Liu, C. Han, Y. Li, Z. Li, Dynamics modeling and residual vibration control of a piezoelectric gripper during wire bonding, IEEE Transactions on Components, Packaging and Manufacturing Technology 7 (12) (2017) 2045–2056.

[42] X. Gao, C. Cao, J. Guo, A. Conn, Elastic electroadhesion with rapid release by integrated resonant vibration, Advanced Materials Technologies 4 (1) (2019) 1800378.

[43] W. Rong, Z. Fan, L. Wang, H. Xie, L. Sun, A vacuum microgripping tool with integrated vibration releasing capability, Review of Scientific Instruments 85 (8) (2014) 085002.

[44] S. Honda, Development of an intelligent vibration gripper, in: G. D. Foret, K. C. Lau, B. O. Nnaji (Eds.), Machine Tool, In-Line, and Robot Sensors and Controls, Vol. 2595, International Society for Optics and Photonics, 1995, pp. 170 – 177.

[45] K. Nakamura, S. Honda, Development of multifinger robot hand with vibration fingers, in: G. D. Foret, K. C. Lau, B. O. Nnaji (Eds.), Machine Tool, In-Line, and Robot Sensors and Controls, Vol. 2595, International Society for Optics and Photonics, SPIE, 1995, pp. 214 – 218.

[46] Y. Suzuki, A. Yamaguchi, S. Nojiri, T. Watanabe, K. Hashimoto, Vibration control for pivoting by robot hand equipped with cavs and fingervision, in: 2021 Fifth IEEE International Conference on Robotic Computing (IRC), 2021, pp. 18–26.

[47] D. E. Welcome, R. G. Dong, X. S. Xu, C. Warren, T. W. McDowell, The effects of vibration-reducing gloves on finger vibration, International Journal of Industrial Ergonomics 44 (1) (2014) 45–59.

[48] D. Karnopp, Computer Simulation of Stick-Slip Friction in Mechanical Dynamic Systems, Journal of Dynamic Systems, Measurement, and Control 107 (1) (1985) 100–103.

[49] A. Sintov, O. Tslil, A. Shapiro, Robotic swing-up regrasping manipulation based on the impulse–momentum approach and clqr control, IEEE Transactions on Robotics 32 (5) (2016) 1079–1090.

[50] J. Slotine, W. Li, Applied Nonlinear Control, Prentice Hall, 1991.

[51] V. Vorotnikov, On the theory of partial stability, Journal of Applied Mathematics and Mechanics 59 (4) (1995) 525–531.

[52] S. Garrido-Jurado, R. Muñoz-Salinas, F. Madrid-Cuevas, M. Marín-Jiménez, Automatic generation and detection of highly reliable fiducial markers under occlusion, Pattern Recognition 47 (6) (2014) 2280–2292.

[53] J. Guo, P. Wu, W. Wang, A precision pose measurement technique based on multi-cooperative logo, Journal of Physics: Conference Series 1607 (1) (2020) 012047.

[54] M. Kalaitzakis, S. Carroll, A. Ambrosi, C. Whitehead, N. Vitzilaios, Experimental comparison of fiducial markers for pose estimation, in: International Conference on Unmanned Aircraft Systems (ICUAS), 2020, pp. 781–789.